PERGAMON

Polyhedron 18 (1999) 3545–3552

POLYHEDRON

www.elsevier.nl/locate/poly

A 'preformed chelate approach' model for coupling amine-modified rhenium and technetium '3+1' mixed ligand complexes to carboxylate residues
Crystal structure of $ReO[CH_3SCH_2CH_2N(CH_2CH_2S)_2][p\text{-}SC_6H_4NH_2]$ and $ReO[CH_3SCH_2CH_2N(CH_2CH_2S)_2][p\text{-}SC_6H_4NHCOC_6H_5]$

Theodosia Maina[a], Charalambos Tsoukalas[a], Georgios Patsis[a], Ioannis Pirmettis[a], Berthold Nock[a], Minas Papadopoulos[a], Catherine Raptopoulou[b], Aris Terzis[b], Efstratios Chiotellis[a,*]

[a]*Institute of Radioisotopes–Radiodiagnostic Products, NCSR 'Demokritos', 15310 Ag. Paraskevi Attikis, Athens, Greece*
[b]*Institute of Materials Science, NCSR 'Demokritos', 15310 Ag. Paraskevi Attikis, Athens, Greece*

Received 7 July 1999; accepted 8 September 1999

Abstract

Selected '3+1' mixed ligand oxorhenium and oxotechnetium complexes containing the SNS/S donor atom set have been modified by introduction of a bifunctional amine anchor on the *p*-position of the thiophenolato monodentate ligand. A representative series of complexes containing several tridentate ligands was prepared both at macromolar (Re complexes) and nanomolar (^{99m}Tc complexes) amounts. Coupling of these complexes to activated carboxylate groups was performed according to the 'preformed chelate approach' using benzoyl chloride as a model molecule. Coupling yields were high both at nanomolar and millimolar metal concentration, as revealed by high-performance liquid chromatographic analysis of ^{99m}Tc and Re species adopting parallel radiometric and photometric detection modes. All Re compounds have been characterized by classical analytical methods. In addition, the structures of representative parent $ReO[CH_3SCH_2CH_2N(CH_2CH_2S)_2][p\text{-}SC_6H_4NH_2]$ and daughter $ReO[CH_3SCH_2CH_2N(CH_2CH_2S)_2][p\text{-}SC_6H_4NHCOC_6H_5]$ complexes were solved by X-ray crystallography. Both compounds adopt a distorted trigonal bipyramidal geometry around rhenium, wherein the oxo group and the sulfur atoms of the SNS ligand occupy the equatorial plane and the nitrogen atom and the sulfur of the monothiol are located at the apical positions *trans* to each other.

Keywords: Mixed ligand approach; Oxotechnetium; Oxorhenium; Preformed chelate approach

1. Introduction

The field of nuclear medicine is expanding toward the early stage diagnosis and therapy of disease at the molecular level. As a result, the demand for effective site-directed molecular probes, that labeled with the appropriate radionuclide will carry the radioactivity selectively to target tissues, is worldwide recognized. For this purpose, efforts are currently focused on the development of novel specific radiopharmaceuticals, e.g. labeled monoclonal antibodies, receptor seeking peptides or bioactive drugs, that can interact efficiently at the molecular level with high affinity low capacity systems in vivo [1–6].

The dominance of ^{99m}Tc radiopharmaceuticals in nuclear medicine practice is based on its ideal nuclear properties ($t_{1/2}$=6 h, gamma photons 140 keV) on the one hand, and its cost effectiveness and wide availability through commercial ^{99}Mo/^{99m}Tc generator systems on the other [1–3,7]. Therefore, a main challenge in radiopharmaceutical design today is the development of highly specific, site-directed ^{99m}Tc probes. However, the incorporation of ^{99m}Tc into a small bioactive molecule is not an easy task as it often requires tethering of a metal chelating agent to its backbone [4–6,8,9]. This coupling proceeds via a bifunctional anchor present on the ligand backbone – often an amine or a carboxylate unit – either after ('preformed chelate approach') or prior to ('post-conjugation approach') complex formation [6,9]. The introduction of the bulky metal chelate has a drastic influence on the

*Corresponding author. Tel.: +30-1-650-3908; fax: +30-1-654-3526.
E-mail address: mainathe@mail.demokritos.gr (E. Chiotellis)

0277-5387/99/$ – see front matter
PII: S0277-5387(99)00286-7

physicochemical characteristics of the bioactive molecule, which is usually small [6]. Several bifunctional chelating agents have been used for coupling to specifically acting compounds, mainly tetradentate ligands suitable for oxotechnetium and oxorhenium [10]. The time consuming synthetic routes involved in the above strategy can be facilitated by the application of bifunctional mixed ligand systems.

In this work we propose the use of representative '3+1' mixed ligand oxotechnetium and oxorhenium complexes of the SNS/S type for coupling to activated carboxylate groups via an amine bifunctional anchor introduced on the common monothiolate ligand. The synthesis and characterization is performed by variation of the tridentate SNS ligand for the following complexes: $ReO[CH_3SCH_2CH_2N(CH_2CH_2S)_2][p\text{-}SC_6H_4NH_2]$, **1**, $ReO[C_2H_5SCH_2CH_2N(CH_2CH_2S)_2][p\text{-}SC_6H_4NH_2]$, **2**, $ReO[(C_2H_5)_2NCH_2CH_2N(CH_2CH_2S)_2][p\text{-}SC_6H_4NH_2]$, **3** and $ReO[C_2H_5N(CH_2CH_2S)_2][p\text{-}SC_6H_4NH_2]$, **4,** as well as for their ^{99m}Tc analogs **1′**, **2′**, **3′** and **4′**. Coupling of the above complexes to activated carboxylate groups is then investigated using C_6H_5COCl as a model molecule according to the 'preformed chelate approach' at both millimolar (Re) and nanomolar (^{99m}Tc) level. The daughter amide complexes thereby formed are: $ReO[CH_3SCH_2CH_2N(CH_2CH_2S)_2][p\text{-}SC_6H_4NHCOC_6H_5]$, **5**, $ReO[C_2H_5SCH_2CH_2N(CH_2CH_2S)_2][p\text{-}SC_6H_4NHCOC_6H_5]$, **6**, $ReO[(C_2H_5)_2NCH_2CH_2N(CH_2CH_2S)_2][p\text{-}SC_6H_4NHCOC_6H_5]$, **7** and $ReO[C_2H_5N(CH_2CH_2S)_2][p\text{-}SC_6H_4NHCOC_6H_5]$, **8**, as well as their ^{99m}Tc counterparts, complexes **5′**, **6′**, **7′** and **8′**. The structure of complexes **1** and **5** as elaborated by X-ray crystallography is also reported.

2. Experimental

2.1. General

Reagent grade chemicals and HPLC solvents were obtained from commercial sources (Fluka, or Aldrich Chemicals), as well as *p*-aminothiophenol and benzoylchloride. Synthesis and purification of $CH_3SCH_2CH_2N(CH_2CH_2SH)_2$, $C_2H_5SCH_2CH_2N(CH_2CH_2SH)_2$, $(C_2H_5)_2NCH_2CH_2N(CH_2CH_2SH)_2$ [11], and $C_2H_5N(CH_2CH_2SH)_2$ [12,13], ligands were performed according to reported protocols. Rhenium was purchased from Aldrich as $KReO_4$ and was converted to the $Re^{V}OCl_3(PPh_3)_2$ precursor according to a described method [14]. Complexes **3** and **4** were available from a previous study [15].

[^{99m}Tc]$NaTcO_4$ was obtained in physiological saline as a commercial $^{99}Mo/^{99m}Tc$ generator eluate (Cis International). Commercial glucoheptonate kits containing a lyophilized mixture of calcium glucoheptonate (200 mg) and $SnCl_2$ (0.2 mg) (Gluco/Demoscan, NCSR 'Demokritos') were used.

IR spectra were recorded as KBr pellets in the range 4000–500 cm^{-1} on a Perkin-Elmer 1600FT-IR spectrophotometer and were referenced to polystyrene. The ^{1}H NMR spectra were recorded on a Bruker FT-NMR/250 AF spectrometer using tetramethyl silane (TMS) as an internal standard. Elemental analyses were performed on a Perkin-Elmer 2400/II automated analyzer. For thin layer chromatography silica gel coated aluminium F_{254} sheets from Merck were used. High performance liquid chromatography (HPLC) analyses were performed on a Waters chromatograph equipped with the 600E solvent delivery system. A LiChrospher 100 RP C-18 (10 μm, 4.0×250 mm) column from Merck was eluted at a flow-rate of 1.0 ml min^{-1} using 2% triethylammonium phosphate (TEAP) buffer pH 7.4/EtOH as the eluent applying the following gradient system: 3 to 20 min from 100 to 30% TEAP buffer; 20 to 30 min 30% TEAP buffer isocratic. Detection of complexes was accomplished by a Waters 991 photodiode array detector (UV trace for Re and the ligands) and a Beckman 171 detector (gamma trace for ^{99m}Tc).

2.2. Synthesis of rhenium complexes

2.2.1. *ReO[CH$_3$SCH$_2$CH$_2$N(CH$_2$CH$_2$S)$_2$][p-SC$_6$H$_4$NH$_2$], **1***

To a 0.5-M AcONa solution in MeOH (4 ml) $Re^{V}OCl_3(PPh_3)_2$ (166.6 mg, 0.2 mmol), $CH_3SCH_2CH_2N(CH_2CH_2SH)_2$ (42 mg, 0.2 mmol) and *p*-aminothiophenol (25 mg, 0.2 mmol) were suspended under stirring. The mixture was refluxed until a clear solution formed. After addition of CH_2Cl_2 the organic phase was washed with H_2O, dried and concentrated to a small volume. Red crystals separated by slow evaporation from CH_2Cl_2/MeOH. Yield: 75 mg (70%). R_f (SiO_2:MeCN:MeOH:CH_2Cl_2:Et_2NH; 75:3.5:15:6.5):0.7; elemental analysis, % found: C, 29.50; H, 4.20; N, 5.65; S, 24.17; % calculated for $C_{13}H_{21}N_2ORES_4$: C, 29.14; H, 3.95; N, 5.23; S, 23.94; UV–Vis (λ_{max}/nm): 259, 447; IR (KBr, ν_{max}/cm^{-1}): 3420, 3337, 2963, 2914, 1621, 1593, 1289, 947 (Re=O str), 823; ^{1}H NMR δ_H (250 MHz, $CDCl_3$, Me_4Si): 2.10 (3H, s, CH_3^*S) 2.86 (2 H, t, $CH_2^*CH_2N$–Re), 2.75–3.00 (4H, m, *exo*, $NCH_2^*CH_2^*S$), 3.45 (2H, m, *endo*, $NCH_2^*CH_2S$), 3.60 (2H, m, *endo*, $NCH_2CH_2^*S$), 3.68 (2H, b, NH_2), 3.93 (2H, t, $CH_2CH_2^*N$–Re), 6.70 (2H, dd, *m*-Ph-H), 7.45 (2H, dd, *o*-Ph-H).

2.2.2. *ReO[C$_2$H$_5$SCH$_2$CH$_2$N(CH$_2$CH$_2$S)$_2$][p-SC$_6$H$_4$NH$_2$], **2***

This complex was prepared by reacting equimolar amounts of $C_2H_5SCH_2CH_2N(CH_2CH_2SH)_2$ (45 mg, 0.2 mmol) and *p*-aminothiophenol (25 mg, 0.2 mmol) on the $Re^{V}OCl_3(PPh_3)_2$ (166.6 mg, 0.2 mmol) precursor in a similar manner as for **1**. Red crystals separated by slow evaporation from CH_2Cl_2/MeOH. Yield: 82 mg (75%). R_f (SiO_2:MeCN:MeOH:CH_2Cl_2:Et_2NH; 75:3.5:15:6.5):0.7; elemental analysis, % found: C, 30.79; H, 4.39; N, 5.65; S, 22.95; % calculated for $C_{14}H_{23}N_2OS_4Re$: C, 30.58; H, 4.22; N, 5.10; S, 23.32; UV–Vis (λ_{max}/nm): 258, 445; IR

(KBr, ν_{max}/cm^{-1}): 3424, 3338, 2953, 2916, 1611, 1593, 1289, 941 (Re=O str), 821; ^{1}H NMR δ_H (250 MHz, $CDCl_3$, Me_4Si): 1.30 (3H, t, $CH_3^*CH_2S$), 2.50–2.90 (6H, m, $CH_3CH_2^*S$, *exo*, $NCH_2^*CH_2^*S$), 3.20–3.55 (4H, m, *endo*, $NCH_2^*CH_2^*S$), 3.67 (2H, b, NH_2), 3.88 (2H, t, $SCH_2CH_2^*N$–Re), 6.65 (2H, dd, *m*-Ph-H), 7.40 (2H, dd, *o*-Ph-H).

2.2.3. *ReO[$CH_3SCH_2CH_2N(CH_2CH_2S)_2$][p-$SC_6H_4NHCOC_6H_5$],* ***5***

To a solution of ReO[$CH_3SCH_2CH_2N(CH_2CH_2S)_2$][*p*-$SC_6H_4NH_2$] (107 mg, 0.2 mmol) and diisopropylethylamine (77.5 mg, 0.6 mmol) in $CHCl_3$ a solution of C_6H_5COCl (112 mg, 0.8 mmol) in $CHCl_3$ was added dropwise under stirring. After 5 min, aliquots of this mixture were analyzed by TLC (SiO_2; MeCN:MeOH:CH_2Cl_2:Et_2NH; 75:3.5:15:6.5) for following the completion of the reaction. The organic phase was washed with H_2O, dried, and concentrated to a small volume. After addition of some EtOH and slow evaporation of the solvents at ambient temperature the product separated as green crystals. Yield: 102 mg (80%). R_f (SiO_2:MeCN:MeOH:CH_2Cl_2:Et_2NH; 75:3.5:15:6.5):0.8; m.p. (from MeOH/CH_2Cl_2): 209–210°C; elemental analysis, % found: C, 37.81; H, 3.72; N, 4.26; S, 19.85; % calculated for $C_{20}H_{25}N_2O_2ReS_4$: C, 37.54; H, 3.94; N, 4.38; S, 20.04; UV–Vis (λ_{max}/nm): 271, 423; IR (KBr, ν_{max}/cm^{-1}): 3373, 2974, 2919, 1664, 1580, 1305, 943 (Re=O str), 831, 707; ^{1}H NMR δ_H (250 MHz, $CDCl_3$, Me_4Si): 2.20 (3H, s, CH_3^*S), 2.92 (2H, t, $SCH_2^*CH_2NRe$), 2.6–3.0 (4H, m, *exo*, $NCH_2^*CH_2^*S$), 3.3–3.6 (4H, m, *endo*, $NCH_2^*CH_2^*S$), 4.0 (2H, t, $SCH_2CH_2^*NRe$), 7.5–7.8 (9H, m, aromatic).

2.2.4. *ReO[$C_2H_5SCH_2CH_2N(CH_2CH_2S)_2$][p-$SC_6H_4NHCOC_6H_5$],* ***6***

To a solution of ReO[$C_2H_5SCH_2CH_2N(CH_2CH_2S)_2$]-[*p*-$SC_6H_4NH_2$] (110 mg, 0.2 mmol) and diisopropylethylamine (77.5 mg, 0.6 mmol) in $CHCl_3$ a solution of C_6H_5COCl (112 mg, 0.8 mmol) in $CHCl_3$ was added and the reaction proceeded in a similar manner as for **5**. Green crystals separated by slow evaporation from $CHCl_3$/EtOH. Yield: 104 mg (80%). R_f (SiO_2:MeCN:MeOH:CH_2Cl_2:Et_2NH; 75:3.5:15:6.5):0.8; elemental analysis, % found: C, 38.77; H, 4.23; N, 4.01; S, 19.22; % calculated for $C_{21}H_{27}N_2O_2ReS_4$: C, 38.57; H, 4.16; N, 4.28; S, 19.61; UV–Vis (λ_{max}/nm): 271, 423; IR (KBr, ν_{max}/cm^{-1}): 3424, 2964, 2925, 2867, 1641, 1584, 943 (Re=O str), 827, 704; ^{1}H NMR δ_H (250 MHz, $CDCl_3$, Me_4Si): 1.2 (3H, t, $CH_3^*CH_2S$), 2.6 (2H, q, $CH_3CH_2^*S$), 2.7–3.0 (4H, mm, *exo*, $NCH_2^*CH_2^*S$), 2.95 (2H, t, $SCH_2^*CH_2NRe$), 3.2–3.5 (4H, mm, *endo*, $NCH_2^*CH_2^*S$), 3.95 (2H, t, $SCH_2CH_2^*NRe$), 7.50–7.90 (9H, m, aromatic).

2.2.5. *ReO[$(C_2H_5)_2NCH_2CH_2N(CH_2CH_2S)_2$][p-$SC_6H_4NHCOC_6H_5$],* ***7***

This complex was prepared by reacting ReO[$C_2H_5NCH_2CH_2N(CH_2CH_2S)_2$][*p*-$SC_6H_4NH_2$] (112 mg, 0.2 mmol) and C_6H_5COCl (112 mg, 0.8 mmol) in a similar manner as for **5**. Green crystals separated by slow evaporation from $CHCl_3$/EtOH. Yield: 113 mg (85%). R_f (SiO_2:MeCN:MeOH:CH_2Cl_2:Et_2NH, 75:3.5:15:6.5):0.8; elemental analysis, % found: C, 41.77; H, 5.00; N, 6.21; S, 14.33%; calculated for $C_{23}H_{32}N_3O_2ReS_3$: C, 41.55; H, 4.85; N, 6.32; S, 14.42%; UV–Vis (λ_{max}/nm): 271, 427, 3259, 2963, 2929, 2800, 1641, 1586, 1288, 942 (Re=O str), 830, 703, 643, ^{1}H NMR δ_H (250 MHz, $CDCl_3$, Me_4Si): 1.05 (6H, t, $CH_3^*CH_2N$), 2.57 (4H, q, $CH_3CH_2^*N$), 2.85 (2H, t, $CH_2^*CH_2N$–Re), 2.75–3.00 (4H, m, *exo*, $NCH_2^*CH_2^*S$), 3.38–3.70 (4H, m, *endo*, $NCH_2^*CH_2^*S$), 3.90 (2H, t, $CH_2CH_2^*N$–Re), 7.50–7.90 (9H, m, aromatic).

2.2.6. *ReO[$C_2H_5N(CH_2CH_2S)_2$][p-$SC_6H_4NHCOC_6H_5$],* ***8***

The complex was prepared by reacting ReO[$C_2H_5N(CH_2CH_2S)_2$][*p*-$SC_6H_4NH_2$] (98 mg, 0.2 mmol) and C_6H_5COCl (112 mg, 0.8 mmol) in a similar manner as for **5**. Green crystals separated by slow evaporation from $CHCl_3$/EtOH. Yield: 95 mg (80%). R_f (SiO_2:MeCN:MeOH:CH_2Cl_2:Et_2NH; 75:3.5:15:6.5):0.8; elemental analysis, % found: C, 38.15; H, 3.10; N, 4.35; S, 16.30; % calculated for $C_{19}H_{23}N_2O_2ReS_3$: C, 38.43; H, 3.90; N, 4.72; S, 16.20; UV–Vis (λ_{max}/nm): 271, 425; IR (KBr, ν_{max}/cm^{-1}): 3291, 2971, 2960, 2927, 1645, 1578, 1288, 941 (Re=O str), 816, 740, 696; ^{1}H NMR δ_H (250 MHz, $CDCl_3$, Me_4Si): 1.40 (3H, t, $CH_3^*CH_2N$), 2.60–2.95 (4H, m, *exo*, $NCH_2^*CH_2^*S$), 3.12–3.65 (4H, m, *endo*, $NCH_2^*CH_2^*S$), 3.95 (2H, q, $CH_3CH_2^*N$–Re), 7.50–7.85 (9H, m, aromatic).

2.3. Synthesis of ^{99m}Tc complexes

The analogous complexes: **1′** ^{99m}TcO[$CH_3SCH_2CH_2N(CH_2CH_2S)_2$][*p*-$SC_6H_4NH_2$], **2′** ^{99m}Tc[$C_2H_5SCH_2CH_2N(CH_2CH_2S)_2$][*p*-$SC_6H_4NH_2$], **3′** ^{99m}Tc[$(C_2H_5)_2NCH_2CH_2N(CH_2CH_2S)_2$] [*p*-$SC_6H_4NH_2$] and **4′** ^{99m}TcO[$C_2H_5N(CH_2CH_2S)_2$][*p*-$SC_6H_4NH_2$] were prepared at the tracer level as previously described for **3′** and **4′** [15]. Briefly, to a centrifuge tube $CH_3SCH_2CH_2N(CH_2CH_2SH)_2$ (4.2 mg, 0.02 mmol) and *p*-aminothiophenol (2.5 mg, 0.2 mmol) were placed and a solution of ^{99m}Tc-glucoheptonate (1.0 ml, 3–10 mCi) was added. The mixture was stirred vigorously on a vortex mixer and was then exctracted in CH_2Cl_2 (3×1.5 ml). The combined organic extracts were dried over $MgSO_4$, which was then filtered off. The radioactivity content of both the aqueous and organic phases was measured separately [Yield (as determined by organic extraction): >85%].

The ^{99m}Tc coupled complexes **5′**, **6′**, **7′**and **8′** were

prepared as follows for **5′**: Complex **1′** was first prepared as described above and then purified by HPLC. The eluent was concentrated to a small volume under a mild stream of nitrogen and transfered into a centrifuge tube, to which C_6H_5COCl (1 mg) was added. The mixture was stirred vigorously on a vortex mixer for 5 min and was then analyzed by HPLC.

HPLC analysis was performed as described above. After co-injection of analogous Re and ^{99m}Tc complexes the corresponding UV/Vis and gamma HPLC profiles were compared.

2.4. X-ray diffraction data and crystal structure determination and refinement

A red (0.10×0.20×0.40 mm) crystal of **1** and a green (0.10×0.15×0.40 mm) of **5** were mounted in air. Diffraction measurements were made on a Crystal Logic Dual Goniometer diffractometer using graphite monochromated Mo Kα radiation. Unit cell dimensions were determined and refined by using the angular settings of 25 automatically centered reflections in the range $11°<2\theta<23°$ and they appear in Table 1. Intensity data were recorded using a θ-2θ scan. For **1**: 2θ max=50°, scan speed 3.5° min^{-1}, scan range $2.4+\alpha_1\alpha_2$ separation; For **5**: 2θ max=50°, scan speed 3.2° min^{-1}, scan range $2.4+\alpha_1\alpha_2$ separation. Three standard reflections monitored every 97 reflections showed less than 3% variation and no decay. Lorentz, polarization and ψ-scan absorption corrections were applied using Crystal Logic software. The structures were solved by direct methods using SHELXS-86 [16] and refined by full-matrix least-squares techniques on F^2 with SHELXL-93 [17]. All hydrogen atoms, in both structures, were located by difference maps and refined isotropically, while all non-H atoms were refined anisotropically. For **1**: reflections collected/unique/used, 3325/3196[R_{int}=0.0255]/3196; parameters refined, 274; [Δ/σ] max=0.020; [$\Delta\rho$] max/[$\Delta\rho$] min=0.622/−0.768 e Å^{-3}; $R1/wR2$ (all data)=0.0327/0.0656. For **5**: reflections collected/unique/used, 4207/4011[R_{int}=0.0080]/4011; parameters refined, 362; [Δ/σ] max=0.005; [$\Delta\rho$] max/[$\Delta\rho$] min=0.518/−0.703 e Å^{-3}; $R1/wR2$ (all data)=0.0171/0.0496.

Table 1
Summary of crystal, intensity collection and refinement data

	Complex **1**	Complex **5**
Formula	$C_{13}H_{21}N_2ORES_4$	$C_{20}H_{25}N_2O_2ReS_4$
Formula weight	535.76	639.86
α (Å)	13.197(7)	9.370(5)
b (Å)	9.695(4)	10.403(6)
c (Å)	14.657(7)	12.883(7)
α (°)		83.58(2)
β (°)	104.69(1)	88.82(2)
γ (°)		66.21(2)
V (Å^3)	1814(1)	1142(1)
Z	4	2
D_{calcd}/D_{measd} (mg m^{-3})	1.962/1.94	1.861/1.84
Space group	$P2_1/n$	P-1
Temperature (K)	298	298
Radiation, λ (Å)	Mo Kα (0.71073)	Mo Kα (0.71073)
Abs. coeff, μ, (mm^{-1})	7.159	5.708
Octants collected	$\pm h, -k, -l$	$\pm h, \pm k, l$
GoF on F^2	1.056	1.048
$R1/wR2$	0.0246/0.0609[a]	0.0160/0.0486[b]

[a] For 2727 reflections with $I>2\sigma(I)$.
[b] For 3840 reflections with $I>2\sigma(I)$.

3. Results and discussion

In this work representative bifunctional oxometal '3+1' mixed ligand complexes of the SNS/S combination were synthesized and characterized both at millimolar (Re complexes **1** and **2**) and nanomolar (^{99m}Tc complexes **1′**–**4′**) concentration. In these compounds a bifunctional amine anchor is introduced on the *para* position of the phenylthiolate coligand. In this way coupling to activated carboxylate residues was pursued using C_6H_5COCl as a model molecule. Thus, the daughter Re complexes **5**–**8** were easily generated under mild conditions from their respective parents (Re complexes **1**–**4**) in millimolar amounts and characterized by classical methods of analysis. Similarly, their ^{99m}Tc counterparts **5′**–**8′** were generated at tracer level from their respective parents and their structure assigned after HPLC chromatographic comparison to the respective Re analogs after adopting parallel radiometric and photometric detection.

The oxorhenium complexes **1**, **2**, **3** and **4** were synthesized by reacting equimolar amounts of tridentate and *p*-aminophenylthiol ligands with $Re^{V}OCl_3(PPh_3)_2$ precursor, as shown in Scheme 1. Given that the thiolate groups are deprotonated upon binding to the MO^{3+} core, neutral complexes are finally produced. Complexes **1** and **2**, are newly synthesized, while the synthesis and chemical characterization of complexes **3** and **4** has been reported elsewhere [15]. Compounds **1** and **2** were purified by extraction in CH_2Cl_2 and slow crystallization from CH_2Cl_2/MeOH. They are crystalline solids, soluble in CH_2Cl_2 and $CHCl_3$, slightly soluble in EtOH and MeOH and insoluble in pentane and water. They are stable in solid state as well as in organic solutions for a period of months. Coupling of complexes **1**, **2**, **3** and **4** with C_6H_5COCl affords the daughter compounds **5**–**8** in high yields, as shown in Scheme 1. The latter were purified by crystallization from $CHCl_3$/EtOH. They are crystalline solids with physicochemical properties similar to those of their parent analogs.

Formation of complexes **1**, **2** and **5**–**8** was established by elemental analysis, IR, UV–Vis and ^{1}H NMR spectroscopies. Thus, they all show an intensive band at 941–947 cm^{-1} assigned to the Re=O stretching vibration. These

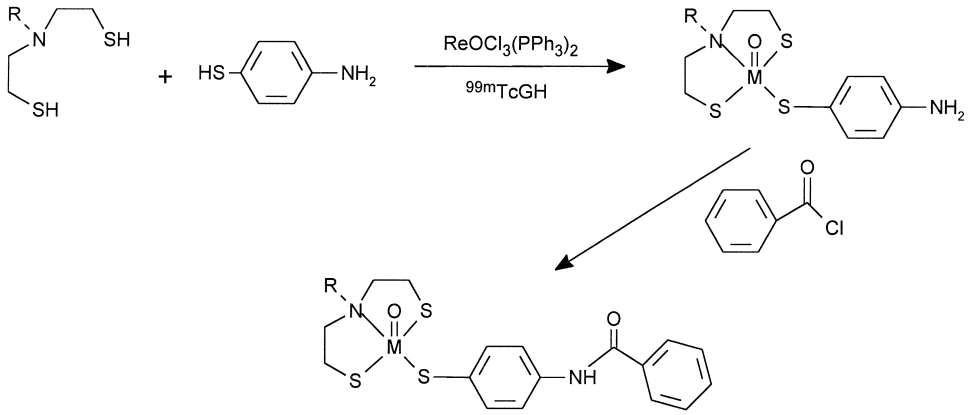

R	M	Parent Complex	Daughter Complex
$CH_3SCH_2CH_2$	Re/^{99m}Tc	**1/1′**	**5/5′**
$C_2H_5SCH_2CH_2$	Re/^{99m}Tc	**2/2′**	**6/6′**
$(C_2H_5)_2NCH_2CH_2$	Re/^{99m}Tc	**3/3′**	**7/7′**
C_2H_5	Re/^{99m}Tc	**4/4′**	**8/8′**

Scheme 1. Preparation of Re and ^{99m}Tc complexes and coupling to C_6H_5COCl.

values are consistent with those reported for several other well-characterized *syn* monooxo complexes of rhenium [18–24]. The aromatic monothiolate coligand is present in the final complexes, as evidenced by the peaks between 821 and 819 cm^{-1}. Complexes **1** and **2** show a double peak in the region 3337–3422 cm^{-1}, characteristic of the primary amine. The presence of the C_6H_5CO-fragment in **5**–**8** complexes is demonstrated on the one hand by the signals between 643 and 742 cm^{-1} and on the other hand by those between 1641 and 1665 cm^{-1} originating from the amide bond. The UV–Vis spectra show maxima at 445 and 448 nm for the parent rhenium complexes and at the range 424–430 nm for the respective amide compounds, characteristic of $Re^{V}O$–S charge transfer band(s), as reported for analogous rhenium complexes [15–21].

The ^{1}H NMR spectra show the expected signals, which can be unambiguously assigned. In particular, all parent ligand peaks – except the three thiolate protons – are found shifted downfield. The deshielding effect of the ReO^{3+} core, due to the anisotropy caused by the circulating electrons of the ReO bond, is related to the distance from the core. Accordingly, the peaks of the vicinal protons are strongly shifted downfield. Moreover the protons, that are *endo* to the ReO core, display a stronger deshielding effect compared to the *exo* protons, as being closer to the core. By coordination the amine substituent may be locked in either a *syn* or an *anti* configuration in respect to the oxometal core and consequently two isomers are theoretically expected. However, correlation of the ^{1}H NMR data to that of reported SNS/S rhenium analogs is easily achieved and is consistent with the formation of only the *syn* isomers in a trigonal bipyramidal array around the metal [15–21]. Complexes **5**–**8** display a more complicated pattern in the aromatic region than the characteristic double of doublets of complexes **1** and **2**, due to the added aromatic ring.

X-ray structure analysis has been performed for complexes **1** and **5** and the pertinent ORTEP diagrams are shown in Figs. 1 and 2, respectively, whereas selected bond distances and angles are listed in Table 2. The coordination geometry about the rhenium atom, in both complexes, is distorted trigonal bipyramidal with the oxo group and the sulfur atoms of the tridentate ligand forming the basal plane and the apical positions occupied by the nitrogen atom and the sulfur of the monodentate thiol. The two complexes correspond to the *syn* isomer with the N-substituent positioned *cis* to the oxo group. The trigonality index, τ, calculated for both compounds is 0.61

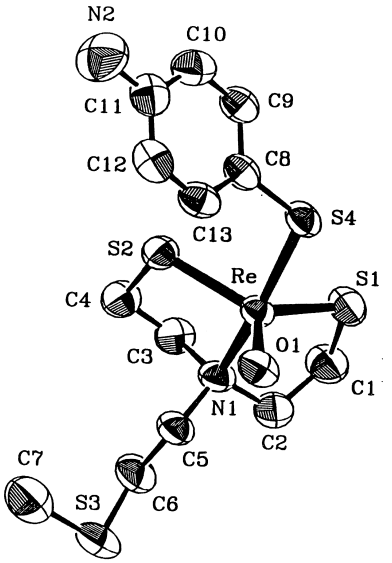

Fig. 1. ORTEP diagram of **1**.

Table 2
Selected bond distances (Å) and angles (°)

	Complex **1**	Complex **5**
Bond distances		
Re–O(1)	1.691(4)	1.704(2)
Re–N(1)	2.205(4)	2.224(3)
Re–S(1)	2.266(2)	2.267(1)
Re–S(2)	2.286(2)	2.290(2)
Re–S(4)	2.299(2)	2.306(1)
Bond angles		
O(1)–Re–N(1)	96.6(2)	94.9(1)
O(1)–Re–S(1)	118.4(2)	119.8(1)
N(1)–Re–S(1)	83.5(1)	83.3(1)
O(1)–Re–S(2)	119.0(1)	119.6(1)
N(1)–Re–S(2)	83.0(1)	83.5(1)
S(1)–Re–S(2)	122.1(1)	119.9(1)
O(1)–Re–S(4)	104.7(1)	104.8(1)
N(1)–Re–S(4)	158.5(1)	160.3(1)
S(1)–Re–S(4)	83.8(1)	88.3(1)
S(2)–Re–S(4)	89.1(1)	85.3(1)

and 0,67 Å for **1** and **5**, respectively. Rhenium is almost coplanar with the atoms of the basal plane of the trigonal bipyramid, lying 0.087 and 0.100 Å out of the plane toward the monodentate thiol, in **1** and **5**, respectively. The torsion angles of the tridentate chelating agent (S1–C1–C2–N1 and N1–C3–C4–S2) are 44.52 and 52.49° for **1** and 44.22 and 53.78° for **5**. The two five-membered rings in the coordination sphere adopt the stable envelope configuration with the carbon atoms adjacent to N1 displaced from the mean plane of the remaining four atoms (displacements 0.57 and 0.65 Å for C2 and C3, respectively, in both structures).

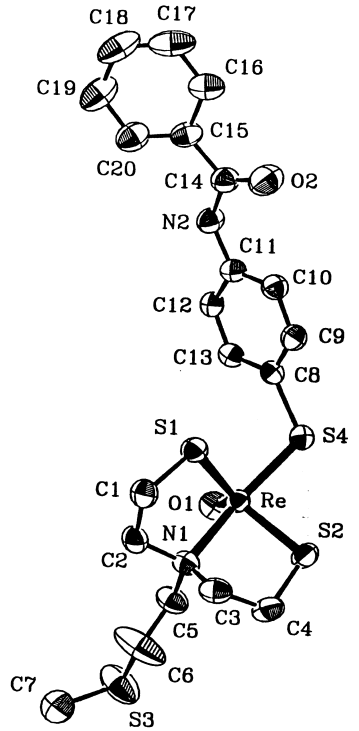

Fig. 2. ORTEP diagram of **5**.

A feature, which should be examined in **5**, is the planarity of the amide unit, which is defined by the torsion angles ω_1 = C–C–N–C, ω_2 = O–C–N–H and ω_3 = O–C–N–C and the values of the calculated parameters $\tau = (\omega_1 + \omega_2)/2(|\omega_1 - \omega_2| < \pi)$, $\chi_N = (\omega_2 - \omega_3 + \pi) \bmod 2\pi$ and $\chi_C = (\omega_1 - \omega_3 + \pi) \bmod 2\pi$, where χ_N and χ_C represent the out-of-plane bending at the amide nitrogen or carbon, respectively [25]. In our case, the three torsion angles ω_1 = C15–C14–N2–C11, ω_2 = O2–C14–N2–HN2 and ω_3 = O2–C14–N2–C11 take the values −167.74, −168.80 and 12.00°, respectively. Thus, the calculated parameters are: $\tau = -168.27°$, $\chi_N = -0.8°$ and $\chi_C = 0.26°$, indicating that the *trans* amide group is planar.

The pendant amine group of the monothiol in **1** is H-bonded to the sulfur atoms S2 and S3 of the tridentate ligand (Table 3) of neighboring complexes and as a result, layers parallel to the diagonal of the *ac* plane are formed. In **5**, the amide hydrogen atom interacts with S2, the coordinated sulfur of the tridentate ligand of a neighboring

Table 3
Hydrogen bond parameters for complexes **1** and **5**[a]

Interaction	D–H (Å)	H . . . A (Å)	D . . . A (Å)	D–H . . . A (°)
Complex **1**				
N2–HN2 . . . S3$^{(i)}$	1.112	2.617	3.697	163.5
N2–HN2 . . . S2$^{(ii)}$	0.843	2.871	3.599	145.7
Complex **5**				
N2–HN2 . . . S2$^{(iii)}$	0.828	3.024	3.839	168.9

[a] Symmetry transformations: (i) $-0.5+x$, $0.5-y$, $-0.5+z$, (ii) $-0.5+x$, $0.5+y$, $0.5-z$, (iii) x, $-1+y$, z.

complex, resulting in the formation of polymeric chains (Table 3).

The analogous ^{99m}Tc complexes **1′**–**4′** were prepared at tracer level by a ligand exchange reaction via ^{99m}Tc-glucoheptonate, as shown in Scheme 1. Labelling yields, as calculated by CH_2Cl_2 extraction of the aqueous reaction mixture, exceeded 85%. The radiochemical purity of the organic extracts was tested by HPLC. Given that the chemistry of Tc and Re are quite similar, corroboration of structure of ^{99m}Tc and Re analogs was achieved by HPLC. By coinjection of respective samples on a reverse phase column both radioactivity (for ^{99m}Tc) and UV–Vis (for Re) traces were identical, demonstrating the formation of isostructural metal species (Fig. 3A,B for complexes **3′** and **3**, respectively).

In order to investigate the efficiency of this method for coupling the above bifunctional ^{99m}Tc complexes to activated carboxylate residues according to the 'preformed chelate approach', C_6H_5COCl was used as a model molecule. Simple incubation of purified parent ^{99m}Tc complexes **1′**–**4′** with C_6H_5COCl in organic medium at ambient temperature resulted in quantitative and rapid formation of daughter compounds, **5′**–**8′**, respectively. Formation of amide complexes was pursued by RP-HPLC as well and a representative radiochromatogram for **7′** is shown in Fig. 3C. The structure of daughter compounds **5′**–**8′** was assigned by coinjection with their respective Re analogs (**5**–**8**) and application of parallel radiometric and photometric detection. As shown in Fig. 3C,D for complexes **7** and **7′** and the pertinent chromatographic profiles are identical, revealing the structural analogy of the compounds.

The above data have shown, that coupling of bifunctional mixed ligand ^{99m}Tc complexes of the SNS/S type to activated carboxylate groups according to the 'preformed chelate approach' is simple and quantitative leading to clearly identified single metal species. As a result, this strategy can be applied for efficiently tagging ^{99m}Tc to pharmacologically interesting target molecules carrying activated carboxylate residues.

Supplementary data

Supplementary data are available from the Cambridge Crystallographic Data Centre, 12 Union Road, Cambridge CB2 1EZ, UK on request, where two CIFs have been deposited with deposition numbers CCDC 127939 and CCDC 127940 for compounds **1** and **5**, respectively.

Acknowledgements

We are grateful to the Agricultural Bank of Greece (ATE) and John Boutaris for financial support to AT and CR.

References

[1] R. Frost, B. Sullivan, The Nuclear Medicine Market, Wiley, New York, 1988.
[2] I. Steigman, W.C. Eckelman, The Chemistry of Technetium in Medicine, National Academy Press, Washington, DC, 1992.
[3] W.C. Eckelman, R.E. Gibson (Eds.), Nuclear Imaging in Drug Discovery, Development and Approval, Birkhäuser, Basel, 1993, p. 113.
[4] S. Jurisson, D. Berning, J. Wei, M. Dangshe, Chem. Rev. 93 (1993) 1137.
[5] W.C. Eckelman, Eur. J. Nucl. Med. 22 (1995) 249.
[6] R.K. Hom, J.A. Katzenellenbogen, Nucl. Med. Biol. 24 (1997) 485.
[7] E.A. Deutsch, K. Libson, S. Jurisson, L.F. Lindoy, Prog. Inorg. Chem. 30 (1983) 75.
[8] K. Schwochau, Angew. Chem., Int. Ed. Engl. 33 (1994) 2258.

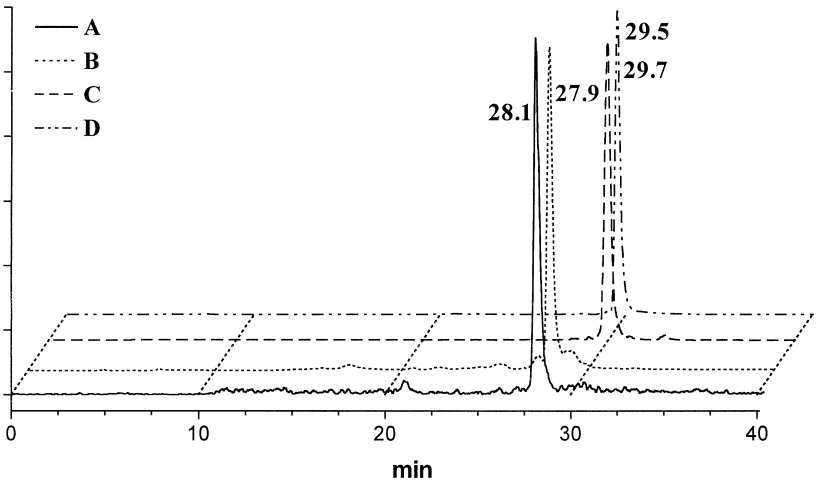

Fig. 3. Radiochromatograms of complexes **3′** (t_R: 28.1 min) and **7′** (t_R: 29.7 min) in A and C, respectively; UV (at 380 nm) chromatograms of complexes **3** (t_R: 27.9 min) and **7** (t_R: 29.5 min) in B and D, respectively.

[9] A. Schaffland, S. Guhlke, F.F.R. Knapp, H.J. Zamora, J. Biersack, J. Label. Compd. Radiopharm. 37 (1995) 493.
[10] W.A. Volkert, in: M. Nicolini, G. Bandoli, U. Mazzi (Eds.), Technetium and Rhenium in Chemistry and Nuclear Medicine, Vol. 4, SG Editoriali, Padova, Italy, 1995, p. 17.
[11] J.L. Corbin, K.E. Miller, N. Pariyadath, S. Wherland, A.E. Bruce, E.I. Stiefel, Inorg. Chim. Acta 90 (1984) 41.
[12] J. Harley-Mason, J. Chem. Soc. (1947) 320
[13] C.P. Marabella, J.H. Enemark, K.F. Miller, A.E. Bruce, N. Pariyadath, J.L. Corbin, E.I. Stiefel, Inorg. Chem. 22 (1983) 3456.
[14] J. Chatt, G.A. Rowe, J. Chem. Soc. (1962) 4019
[15] M. Papadopoulos, C. Tsoukalas, I. Pirmettis, B. Nock, T. Maina, Z. Abedin, C. Raptopoulou, A. Terzis, E. Chiotellis, Inorg. Chim. Acta 285 (1999) 97.
[16] G.M. Sheldrick, SHELXS-86: Structure Solving Program, University of Göttingen, Germany, 1986.
[17] G.M. Sheldrick, SHELXL-93: Crystal Structure Refinement, University of Göttingen, Germany, 1993.
[18] T.N. Rao, D. Adhikesavalu, A. Camerman, A.R. Fritzberg, J. Am. Chem. Soc. 112 (1990) 5798.
[19] L.C. Francesconi, G. Graczyk, S. Wehrli, N. Shaikh, D. McClinton, S. Liu, J. Zubieta, H.F. Kung, Inorg. Chem. 32 (1993) 3114.
[20] J. O'Neil, S. Wilson, J. Katzenellenbogen, Inorg. Chem. 33 (1994) 319.
[21] M. Papadopoulos, I. Pirmettis, M. Pelecanou, C.P. Raptopoulou, A. Terzis, C.I. Stassinopoulou, E. Chiotellis, Inorg. Chem. 35 (1996) 7377.
[22] H. Spies, T. Fietz, H. Pietzsch, B. Johannsen, P. Leibnitz, G. Reck, D. Scheller, K. Klostermann, J. Chem. Soc., Dalton Trans. (1995) 227
[23] M. Papadopoulos, I. Pirmettis, C. Raptopoulou, A. Terzis, E. Chiotellis, in: U. Mazzi, G. Bandoli, M. Nicolini (Eds.), Technetium and Rhenium in Chemistry and Nuclear Medicine, Vol. 4, SGE, Padova, 1995, p. 223.
[24] H. Spies, T. Fietz, M. Glaser, H.J. Pietzsch, B. Johannsen, in: U. Mazzi, G. Bandoli, M. Nicolini (Eds.), Technetium and Rhenium in Chemistry and Nuclear Medicine, Vol. 4, SGE, Padova, 1995, p. 243.
[25] F.K. Winkler, J.D. Dunitz, J. Mol. Biol. 59 (1971) 169.